Letter

Significance of tensor force in pseudospin symmetry

H. Nakada [1,2,*] and T. Inakura [3,4,†]

[1]*Department of Physics, Graduate School of Science, Chiba University, Yayoi-cho 1-33, Inage, Chiba 263-8522, Japan*

[2]*Research Center for Nuclear Physics, Osaka University, Mihogaoka 10-1, Ibaraki, Osaka 567-0047, Japan*

[3]*Office of Institutional Research and Decision Support, Tokyo Institute of Technology, Meguro, Tokyo 152-8550, Japan*

[4]*Laboratory for Zero-Carbon Energy, Institute of Innovative Research, Tokyo Institute of Technology, Meguro, Tokyo 152-8550, Japan*

(Received 2 July 2024; accepted 22 October 2024; published 7 November 2024)

We point out that the pseudospin symmetry (PSS) of nuclei significantly depends on the proton (Z) and neutron numbers (N), sometimes giving rise to characteristic structures. By using the nonrelativistic spherical Hartree-Fock calculation with a realistic tensor force, we show that the tensor force may be deeply relevant to the Z and N dependence of the PSS. While the PSS has often been discussed in the context of relativistic symmetry, the tensor-force effects on the PSS sometimes look analogous to the Z and N dependence of the PSS in relativistic mean-field (RMF) calculations without explicit tensor force. The observed variation of the $p0d_{3/2}$-$p1s_{1/2}$ levels from ^{40}Ca to ^{34}Si is consistent with the tensor-force-driven Z dependence of the PSS, but not necessarily with the RMF result. The present analysis elucidates the significance of the tensor force when discussing the PSS.

DOI: 10.1103/PhysRevC.110.L051301

Introduction. Various symmetries have been found and discussed in nuclear structure physics. The pseudospin symmetry (PSS) [1,2] is among them, being crucial for some characteristic structures as discussed below. The so-called pseudo-LS coupling scheme and the pseudo-SU(3) model were also proposed on top of the PSS [1]. In short, the PSS is the near degeneracy between $(n, \ell, j = \ell + 1/2)$ and $(n' = n - 1, \ell' = \ell + 2, j' = \ell' - 1/2)$ single-particle (s.p.) orbitals found in a certain region of the nuclear chart, where (n, ℓ, j) stands for the radial, orbital, and summed angular-momentum quantum numbers. For those pairs, the pseudoradial and orbital quantum numbers are assigned as $\tilde{n} = n - 1 = n'$ and $\tilde{\ell} = \ell + 1 = \ell' - 1$. It has been argued since the late 1990s that the PSS is a relativistic symmetry [3–5], as $\tilde{\ell}$ is the real orbital angular momentum of the lower component of the Dirac spinor, rather than a hypothetical quantum number.

The tensor force has been pointed out to give rise to proton-(Z) and neutron-number (N) dependence of the shell structure [6–9], which is sometimes called "shell evolution." This Z and N dependence of the shell structure should be relevant to the PSS. Whereas tensor-force effects on the PSS have been argued [10], sufficient attention has not been paid to the Z and N dependence. In this paper, we discuss how the tensor force affects the PSS, with particular interest in the variation due to the occupation of specific orbits.

We apply the spherical Hartree-Fock (HF) calculations, and compare the s.p. energy spacings between the PSS partners among effective interactions (or energy-density functionals) with and without the tensor force. Because the tensor force is active in jj-closed configurations while inactive under the spin saturation [11], the variation of the spacings between an ℓs-closed nucleus and a jj-closed one provides a good indication of the tensor-force effects. In investigating the tensor-force effects, the M3Y-type semirealistic interaction [12] has a desirable property. It contains a realistic tensor force, which has been derived from a bare nucleonic interaction through the G-matrix [13] without further adjustment, and at the same time the strength of the tensor force is well examined in the shell structure [14]. We calculate s.p. energies with the M3Y-P6 interaction [15,16], which provides the magic numbers compatible with most experimental data up to unstable nuclei [9]. They are compared with those of the Gogny-D1S interaction [17], which is a representative of the phenomenological interactions that have been used for a variety of nuclear structure studies with no explicit tensor force. To clarify the tensor-force effects, we also present the s.p. energies obtained with M3Y-P6 but after subtracting the contribution of the tensor force. The s.p. levels in the relativistic mean-field (RMF) approach with the DD-ME2 parameter-set [18] are shown as well, for which the DIRHB code [19] has been employed. Note that, under the time-reversal symmetry, the tensor force has contributions only from the exchange terms [11,20,21], which are not included in the RMF calculations. Experimental information on the s.p. levels can be obtained from the low-lying levels adjacent to the doubly closed nuclei. Despite the fragmentation of the s.p. strengths, the energy difference between the lowest-lying states is often an acceptable measure, particularly within a single nuclide. We shall compare the calculated levels with the available experimental results.

*Contact author: nakada@faculty.chiba-u.jp

†Contact author: inakura@gmail.com

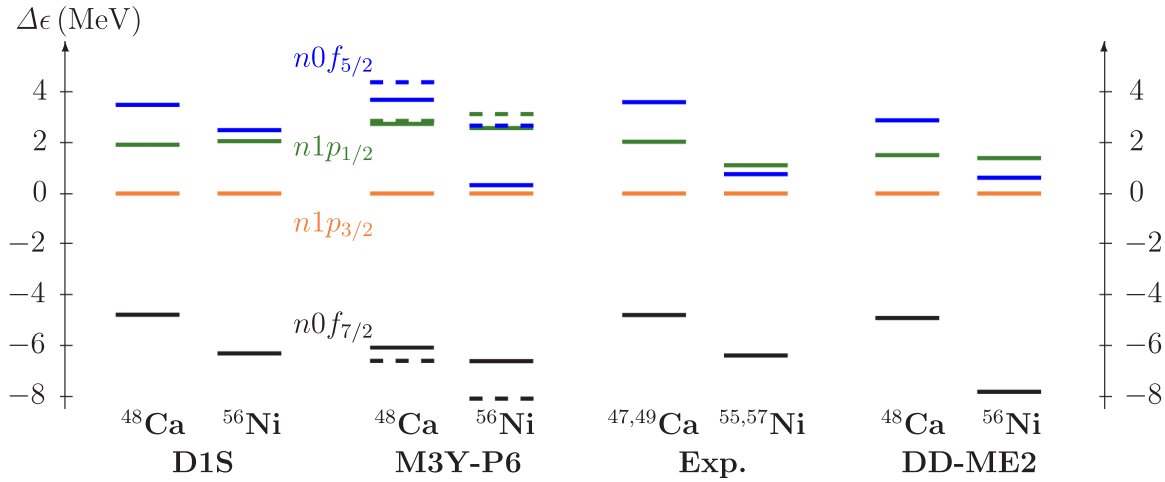

FIG. 1. Single-particle energy of $n0f_{5/2}$ (blue bars) measured from its PSS partner $n1p_{3/2}$ (orange bars) at ^{48}Ca and ^{56}Ni. The spherical HF results with D1S and M3Y-P6 are depicted. The result after subtracting the tensor-force contribution from that with M3Y-P6 is shown by the dashed bars, and the RMF result with DD-ME2 is also presented. Energies of $n0f_{7/2}$ (black bars) and $n1p_{1/2}$ (green bars) are also displayed for reference. For comparison, the measured energies of ^{49}Ca and ^{57}Ni of the lowest levels with corresponding spin-parities [24] are plotted. For $n0f_{7/2}$, the reference energy is extracted from the binding energies of ^{47}Ca and ^{55}Ni [25].

Z and N dependence of pseudospin symmetry. While the PSS plays important roles in nuclear structure, we here point out that the PSS has Z and N dependence, well maintained in certain regions but almost lost in others. In discussing the origin of the PSS, the Z and N dependence should not be discarded.

At the mean-field level, the tensor force has the following effects [6–9,11,16]. It predominantly acts between a proton and a neutron. At the ℓs closure, the tensor-force effects become negligibly small owing to the spin saturation. When a proton (neutron) orbit with $j = \ell + 1/2$ is occupied, the tensor force pushes up neutron (proton) $j' = \ell' + 1/2$ orbits and pushes down neutron (proton) $j' = \ell' - 1/2$ orbits. Thus, the tensor force yields significant Z and N dependence of the s.p. level spacings through the occupation of specific orbitals.

We first look at the neutron shell structure above $N = 28$. The near degeneracy of $n0f_{5/2}$ and $n1p_{3/2}$ in the Ni nuclei is a typical example of the PSS [1]. On the other hand, the magicity of $N = 32$ near ^{52}Ca [22] occurs due to the large spacing between these orbits, implying that the PSS significantly depends on the proton number Z. In Fig. 1, the calculated s.p. energy spacing between the PSS partners at ^{48}Ca is compared with the spacing at ^{56}Ni. Occupation of protons on $p0f_{7/2}$ gives rise to the difference between ^{48}Ca and ^{56}Ni. This Z dependence of the shell structure may largely be ascribed to the tensor force [23]. The tensor force is active at ^{56}Ni owing to the occupation on $p0f_{7/2}$, while its effect is small at ^{48}Ca because of the ℓs-closure for protons. The Z dependence in the M3Y-P6 result is compatible with the experimental levels extracted from the lowest levels at ^{49}Ca and ^{57}Ni. In contrast, D1S does not give the Z dependence accounting for the PSS around the Ni nuclei. If we subtract the tensor-force contribution, M3Y-P6 reaches quite a similar result to that of D1S as shown by the dashed bars in Fig. 1, confirming that the tensor force is responsible for the Z dependence. In all examples handled in this paper, the s.p. spacings with M3Y-P6 resemble those with D1S if subtracting the tensor-force contribution.

Intriguingly, the RMF result with DD-ME2 also describes the Z dependence. Without the exchange terms, the origin of the Z dependence in the DD-ME2 result should be attributed to the central channel. When we look at the calculated $n0f_{7/2}$ level together with $n0f_{5/2}$ and $n1p_{3/2}$, we find that both $n0f_{7/2}$ and $n0f_{5/2}$ shift down from ^{48}Ca to ^{56}Ni in the DD-ME2 result, almost keeping the spacing between them. Thus, the Z dependence of the PSS in the DD-ME2 result originates from the different Z dependence among the s.p. levels with different ℓ values, not greatly varying the ℓs splitting. This is a sharp contrast to the M3Y-P6 result. Similar behavior is found in other regions shown below. If we extract the s.p. energies from the measured binding energies of ^{47}Ca and ^{55}Ni, the variation of the $n0f_{7/2}$ level is in between the M3Y-P6 and DD-ME2 results. Considering together the ambiguity in extracting the s.p. energies due to the fragmentation of the s.p. states, these data cannot conclusively indicate a preference between the tensor-force picture and the relativistic picture of the Z dependence.

The relative position of $n1p_{1/2}$ is also displayed in Fig. 1. The $1/2^-$ level lies close to $3/2^-$ and $5/2^-$ experimentally. The position of the $1/2^-$ level does not appear to be well reproduced at ^{56}Ni in the D1S and M3Y-P6 results. However, our main concern is the Z dependence of the level spacing. The spacing between $n1p_{3/2}$ and $n1p_{1/2}$ does not change much from ^{48}Ca to ^{56}Ni in all the results, although it slightly widens in the D1S and tensor-subtracted M3Y-P6 results, opposite to the experimental data.

Let us turn to other cases. Whereas the $p1s_{1/2}$ level lies well below its PSS partner $p0d_{3/2}$ near ^{40}Ca, the two levels are inverted and close lying around ^{48}Ca, giving an example of the N dependence of the PSS. It has been pointed out that the energy difference of these s.p. levels is governed by the tensor force [14]. The role of the tensor force is again confirmed

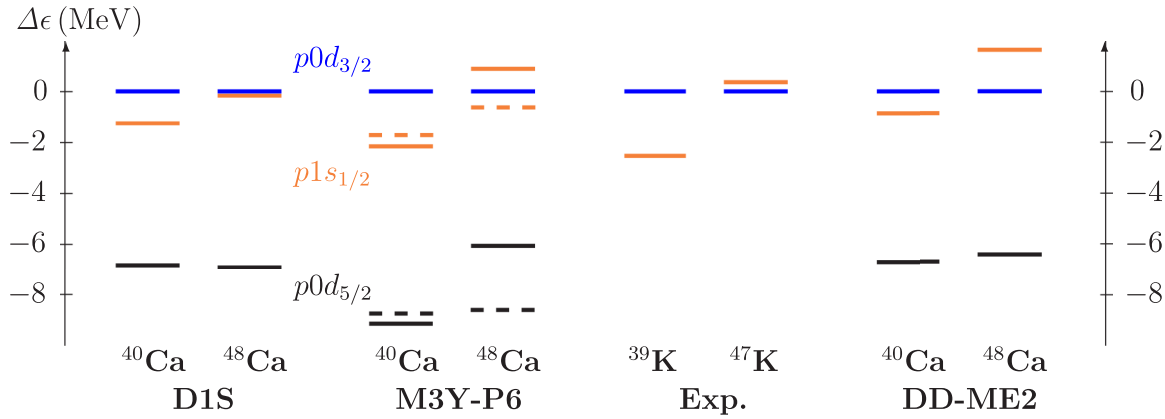

FIG. 2. Single-particle energy of $p1s_{1/2}$ (orange bars) measured from its PSS partner $p0d_{3/2}$ (blue bars) at ^{40}Ca and ^{48}Ca. Energy of $p0d_{5/2}$ (black bars) is also displayed. The measured energies of ^{39}K and ^{47}K [24] are shown for comparison. See Fig. 1 for other conventions.

in Fig. 2, in which the variation of the energy spacing between $p0d_{3/2}$ and $p1s_{1/2}$ from ^{40}Ca to ^{48}Ca is shown. The tensor-force effect is sizable at ^{48}Ca owing to the occupation on $n0f_{7/2}$, while it is small at ^{40}Ca. The experimental levels are extracted from the lowest levels of ^{39}K and ^{47}K with corresponding spin-parity. The energy difference is similar to the one obtained from the proton knockout reaction data, which almost exhaust the spectroscopic factors [26,27]. The variation of the difference between $p0d_{3/2}$ and $p1s_{1/2}$ is insufficient in the RMF result [28,29]. Notable difference is found between the full M3Y-P6 result and the others in the variation of $p0d_{5/2}$ from ^{40}Ca to ^{48}Ca, reflecting the tensor force, though the energy of this deep hole state is not easy to evaluate from experimental data because of its fragmentation.

The $E2$ excitation strengths in the neutron-deficient Sn nuclei are hardly described as far as the stiff spherical shape is assumed for their ground states [30,31]. The near degeneracy of the PSS partners $n0g_{7/2}$ and $n1d_{5/2}$ seems to trigger their deformability. In contrast, $N = 56$ may be a submagic number at ^{96}Zr [9,32], whose excitation energy is relatively high [24]. The $n0g_{7/2}$ level is distant from $n1d_{5/2}$ at Zr but becomes close as $p0g_{9/2}$ is occupied, providing another example of the Z dependence of the PSS. We investigate the Z dependence of the s.p. level spacing by picking up the $N = 50$ nuclei. As observed in Fig. 3, M3Y-P6 well describes the experimental Z dependence, owing to the tensor force. The level spacing between $n0g_{7/2}$ and $n1d_{5/2}$ seems too large at Sn with D1S and too small at Zr with DD-ME2. Although the variation of $n0g_{9/2}$ is distinguished between M3Y-P6 and the others, data on ^{99}Sn, which lies outside the proton drip line, are required to access it experimentally.

Via the measurements of the isotope shifts, the differential charge radii have been extracted with high precision. Apart from exceptions like the neutron-deficient Sn nuclei mentioned above, the proton configuration hardly changes in magic-Z isotopes, e.g., Pb, Sn, Ni, and Ca. It has been shown that the charge radii prevalently have kinks at magic N [33–36]. For Pb, the near degeneracy of the PSS partners $n0i_{11/2}$ and $n1g_{9/2}$ was argued to be one of the key ingredients providing the kink at ^{208}Pb [37–41]. The near degeneracy of $n0h_{9/2}$ and $n1f_{7/2}$ could be important [42] in the newly discovered kink at ^{132}Sn [35], as well. It is noted that not all RMF parameter sets successfully reproduce the kink at ^{132}Sn, which is possibly related to the degree of the PSS [43]. In Fig. 4, the variation of the energy spacing between $n0h_{9/2}$ and $n1f_{7/2}$ from ^{140}Ce to ^{132}Sn is presented. At ^{140}Ce, $p0g_{7/2}$ is fully occupied in the calculated results, making the tensor-force effect on the neutron orbitals vanishingly small. As the observed excitation energy is relatively high [24], $Z = 58$ could be a submagic number at ^{140}Ce [9] in reality. The $n0h_{9/2}$ orbit lies above $n1f_{7/2}$ at ^{140}Ce, and it goes up further at ^{132}Sn. However, the tensor force suppresses the increase of the $n0h_{9/2}$ energy, keeping the PSS a good approximation and producing a kink at ^{132}Sn via a three-nucleon-force effect [42], whereas another study ascribes the origin of the kink to the property of the pairing [44]. Analogously, the PSS maintained by the tensor force is important for the kink of the charge radii at ^{208}Pb.

Let us go back to the region near ^{40}Ca. The $n1s_{1/2}$ orbit lies below its PSS partner $n0d_{3/2}$. It may go up and down as $p0d_{3/2}$ becomes unoccupied. D1S and DD-ME2, which do not contain explicit tensor force, predict that $n1s_{1/2}$ goes down from ^{40}Ca to ^{34}Si, while M3Y-P6 gives the opposite trend. These qualitatively different predictions are noteworthy, because they seem distinctive of the tensor-force effect. The ^{34}Si nucleus is expected to have a doubly-magic nature, with a good possibility of the proton semibubble density [14,45]. Therefore, experimental data at ^{39}Ca and ^{33}Si could supply a reference. As shown in Fig. 5, the measured energies of the lowest levels are consistent with the M3Y-P6 result.

We have discussed variations of the s.p. level spacings between the pseudospin partners through the occupation of specific orbits. One might expect that a long chain of isotopes or isotones gives clear indication of tensor-force effects in the PSS, possibly discriminating them from the relativistic effects. In Figs. 14, 15, and 16 of Ref. [46], the variation of the s.p. level spacing was investigated for the chains of $Z = 50$, $N = 50$, and $N = 82$ nuclei, respectively. To elucidate the roles of the tensor force, results of the nonrelativistic interactions with and without tensor force were compared. However, the central channels in the interaction, which are more or less

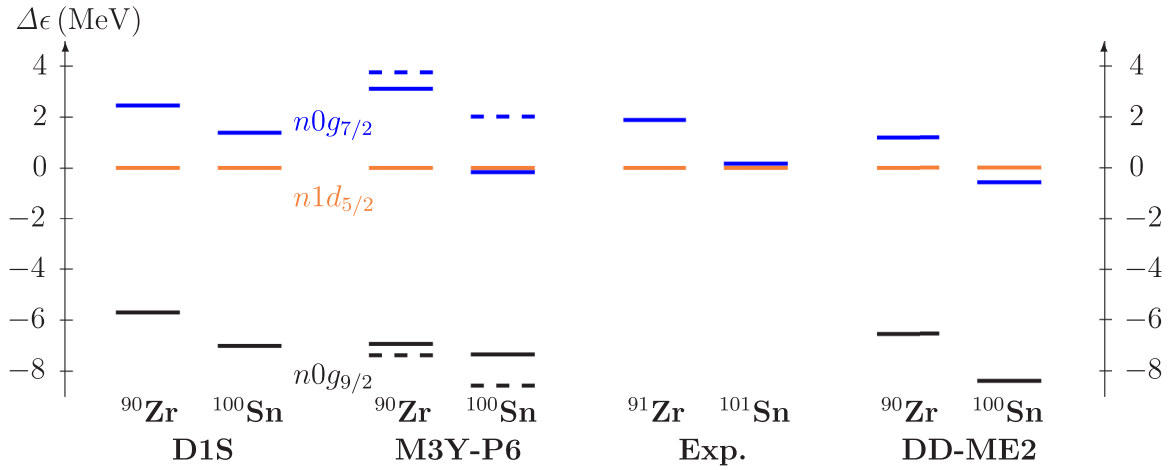

FIG. 3. Single-particle energy of $n0g_{7/2}$ (blue bars) measured from its PSS partner $n1d_{5/2}$ (orange bars) at ^{90}Zr and ^{100}Sn. Energy of $n0g_{9/2}$ (black bars) is also displayed. The measured energies of ^{91}Zr and ^{101}Sn [24] are shown for comparison. See Fig. 1 for other conventions.

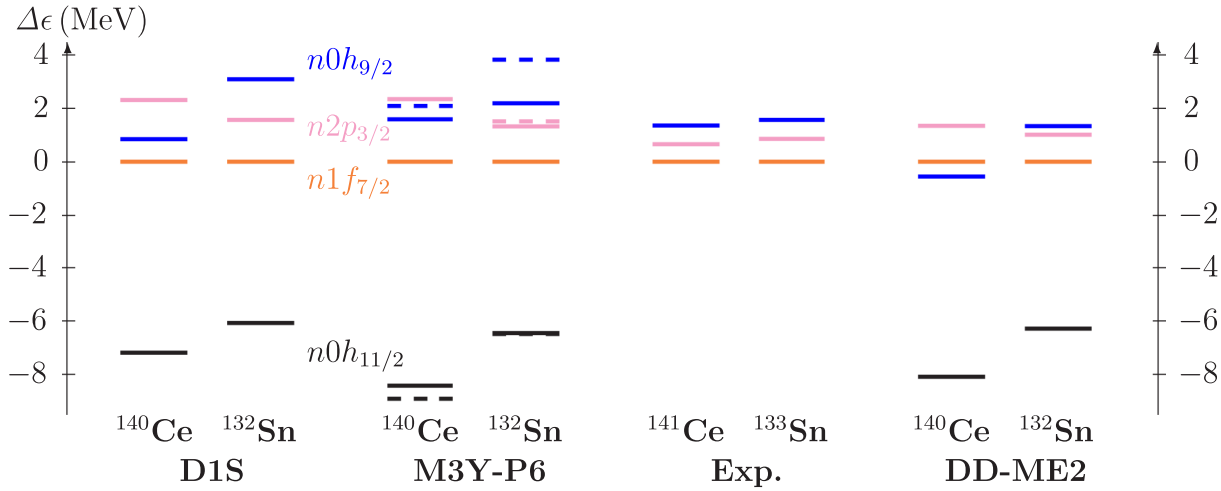

FIG. 4. Single-particle energy of $n0h_{9/2}$ (blue bars) measured from its PSS partner $n1f_{7/2}$ (orange bars) at ^{140}Ce and ^{132}Sn. Energies of $n0h_{11/2}$ (black bars) and $n2p_{3/2}$ (lavender bars) are also displayed. The measured energies of ^{141}Ce and ^{133}Sn [24] are shown for comparison. See Fig. 1 for other conventions.

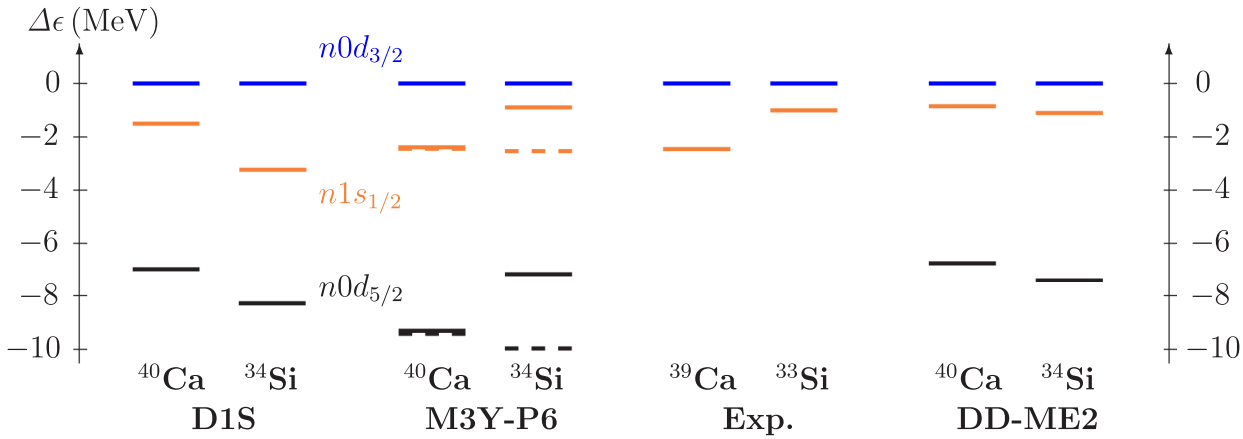

FIG. 5. Single-particle energy of $n1s_{1/2}$ (orange bars) measured from its PSS partner $n0d_{3/2}$ (blue bars) at ^{40}Ca and ^{34}Si. Energy of $n0d_{5/2}$ (black bars) is also displayed. The measured energies of ^{39}Ca and ^{33}Si [24] are shown for comparison. See Fig. 1 for other conventions.

adjusted to experimental data, also influence the level spacing, and obscure the tensor-force effects on the PSS in the chains, whereas the tensor force significantly influences the relative energies of the unique-parity orbits. We have confirmed that this holds for the DD-ME2 case.

Summary and discussion. We have pointed out the relevance of the Z and N dependence of the shell structure, often called "shell evolution," to the pseudospin symmetry (PSS). This indicates that the tensor force may play a significant role in the PSS. We have investigated the tensor-force effects on the PSS by employing the spherical Hartree-Fock calculations with M3Y-P6. It should be noted that the tensor force is undoubtedly contained in the nucleonic interaction, and the tensor force adopted here is a realistic one derived from the G-matrix. We find that the tensor-force effects on the PSS sometimes look analogous to the Z and N dependence of the PSS in the relativistic mean-field (RMF) calculations without explicit tensor force, despite difference in the physics origin. However, for the variation of the $p0d_{3/2}$-$p1s_{1/2}$ levels from ^{40}Ca to ^{34}Si, the experimental data is compatible with the tensor-force-driven picture of the PSS, but not with the prediction of the RMF with the DD-ME2 Lagrangian. Although it is too early to conclude from this case that the tensor force dominates the Z and N dependence of the PSS, it demonstrates that the tensor force may be significant in the PSS. Conversely, it could be misleading to discuss the PSS only within the context of relativistic symmetry without paying attention to the tensor-force effects.

The tensor force between nucleons arises in the relativistic Hartree-Fock (RHF) framework [47,48], which takes account of the exchange terms. The role of the tensor coupling due to the ρ-meson in the PSS has been argued [49], which gives a part of the tensor-force effect discussed here. See Ref. [21] for the relation of the meson-nucleon coupling in the RHF to the nucleonic tensor force. As the tensor force and the relativistic effects may affect the PSS cooperatively and competitively, it is of interest to view how the Z and N dependence of the PSS arises within the RHF scheme.

Acknowledgments. Discussions with N. Hinohara and T. Naito are gratefully acknowledged. This work is supported by the JSPS KAKENHI, Grant No. JP24K07012. Some of the numerical calculations were performed on HITAC SR24000 at Institute of Management and Information Technologies at Chiba University.

[1] A. Arima, M. Harvey, and K. Shimizu, Phys. Lett. B **30**, 517 (1969).
[2] K. T. Hecht and A. Adler, Nucl. Phys. A **137**, 129 (1969).
[3] J. N. Ginocchio, Phys. Rev. Lett. **78**, 436 (1997).
[4] J. Meng, K. Sugawara-Tanabe, S. Yamaji, P. Ring, and A. Arima, Phys. Rev. C **58**, R628 (1998).
[5] H. Liang, J. Meng, and S.-G. Zhou, Phys. Rep. **570**, 1 (2015).
[6] T. Otsuka, T. Suzuki, R. Fujimoto, H. Grawe, and Y. Akaishi, Phys. Rev. Lett. **95**, 232502 (2005).
[7] T. Lesinski, M. Bender, K. Bennaceur, T. Duguet, and J. Meyer, Phys. Rev. C **76**, 014312 (2007).
[8] H. Sagawa and G. Colò, Prog. Part. Nucl. Phys. **76**, 76 (2014).
[9] H. Nakada and K. Sugiura, Prog. Theor. Exp. Phys. **2014**, 33D02 (2014).
[10] Y. Z. Wang, G. L. Yu, Z. Y. Li, and J. Z. Gu, J. Phys. G **40**, 045105 (2013).
[11] Y. Suzuki, H. Nakada, and S. Miyahara, Phys. Rev. C **94**, 024343 (2016).
[12] H. Nakada, Phys. Rev. C **68**, 014316 (2003).
[13] N. Anantaraman, H. Toki, and G. F. Bertsch, Nucl. Phys. A **398**, 269 (1983).
[14] H. Nakada, K. Sugiura, and J. Margueron, Phys. Rev. C **87**, 067305 (2013).
[15] H. Nakada, Phys. Rev. C **87**, 014336 (2013).
[16] H. Nakada, Int. J. Mod. Phys. E **29**, 1930008 (2020).
[17] J. F. Berger, M. Girod, and D. Gogny, Comput. Phys. Commun. **63**, 365 (1991).
[18] G. A. Lalazissis, T. Nikšić, D. Vretenar, and P. Ring, Phys. Rev. C **71**, 024312 (2005).
[19] T. Nikšić, N. Paar, D. Vretenar, and P. Ring, Comput. Phys. Commun. **185**, 1808 (2014).
[20] D. Vautherin and D. M. Brink, Phys. Rev. C **5**, 626 (1972).
[21] Z. Wang, Q. Zhao, H. Liang, and W. H. Long, Phys. Rev. C **98**, 034313 (2018).
[22] J. I. Prisciandaro, P. F. Mantica, B. A. Brown, D. W. Anthony, M. W. Cooper, A. Garcia, D. E. Groh, A. Komives, W. Kumarasiri, P. A. Lofy *et al.*, Phys. Lett. B **510**, 17 (2001).
[23] H. Nakada, Phys. Rev. C **81**, 051302(R) (2010).
[24] http://www.nndc.bnl.gov/nudat3/.
[25] M. Wang, W. J. Huang, F. G. Kondev, G. Audi, and S. Naimi, Chin. Phys. C **45**, 030003 (2021).
[26] P. Doll, G. J. Wagner, K. T. Knöpfle, and G. Mairle, Nucl. Phys. A **263**, 210 (1976).
[27] C. A. Ogilvie, D. Barker, J. B. A. England, M. C. Mannion, J. M. Nelson, L. Zybert, and R. Zybert, Nucl. Phys. A **465**, 445 (1987).
[28] M. Grasso, Z. Y. Ma, E. Khan, J. Margueron, and N. Van Giai, Phys. Rev. C **76**, 044319 (2007).
[29] Y. Z. Wang, J. Z. Gu, X. Z. Zhang, and J. M. Dong, Phys. Rev. C **84**, 044333 (2011).
[30] T. Togashi, Y. Tsunoda, T. Otsuka, N. Shimizu, and M. Honma, Phys. Rev. Lett. **121**, 062501 (2018).
[31] Y. Omura, H. Nakada, K. Abe, and M. Takahashi, Phys. Rev. C **108**, 054308 (2023).
[32] S. Miyahara and H. Nakada, Phys. Rev. C **98**, 064318 (2018).
[33] I. Angeli and K. P. Marinova, At. Data Nucl. Data Tables **99**, 69 (2013).
[34] R. F. Garcia Ruiz, M. L. Bissell, K. Blaum, A. Ekström, N. Frömmgen, G. Hagen, M. Hammen, K. Hebeler, J. D. Holt *et al.*, Nat. Phys. **12**, 594 (2016).
[35] C. Gorges, L. V. Rodríguez, D. L. Balabanski, M. L. Bissell, K. Blaum, B. Cheal, R. F. Garcia Ruiz, G. Georgiev, W. Gins *et al.*, Phys. Rev. Lett. **122**, 192502 (2019).
[36] H. Nakada, Phys. Rev. C **100**, 044310 (2019).
[37] M. M. Sharma, G. Lalazissis, J. König, and P. Ring, Phys. Rev. Lett. **74**, 3744 (1995).
[38] P.-G. Reinhard and H. Flocard, Nucl. Phys. A **584**, 467 (1995).

[39] P. M. Goddard, P. D. Stevenson, and A. Rios, Phys. Rev. Lett. **110**, 032503 (2013).
[40] H. Nakada and T. Inakura, Phys. Rev. C **91**, 021302(R) (2015).
[41] T. Day Goodacre, A. V. Afanasjev, A. E. Barzakh, B. A. Marsh, S. Sels, P. Ring, H. Nakada, A. N. Andreyev, P. Van Duppen, N. A. Althubiti *et al.*, Phys. Rev. Lett. **126**, 032502 (2021).
[42] H. Nakada, Phys. Rev. C **92**, 044307 (2015).
[43] T. Naito, T. Oishi, H. Sagawa, and Z. Wang, Phys. Rev. C **107**, 054307 (2023).
[44] S. A. Fayans, S. V. Tolokonnikov, E. L. Trykov, and D. Zawischa, Nucl. Phys. A **676**, 49 (2000).
[45] J. J. Li, W. H. Long, J. L. Song, and Q. Zhao, Phys. Rev. C **93**, 054312 (2016).
[46] H. Nakada, Phys. Rev. C **78**, 054301 (2008).
[47] A. Bouyssy, J.-F. Mathiot, N. Van Giai, and S. Marcos, Phys. Rev. C **36**, 380 (1987).
[48] W. H. Long, H. Sagawa, N. V. Giai, and J. Meng, Phys. Rev. C **76**, 034314 (2007).
[49] J. Geng, J. J. Li, W. H. Long, Y. F. Niu, and S. Y. Chang, Phys. Rev. C **100**, 051301(R) (2019).